

Factors Controlling in the Concentration of Gold, Uranium and some Base Metals in the Lower Carboniferous Marl at Wadi El Kharig area, Southwestern Sinai, Egypt

Osama R. Sallam

Nuclear Materials Authority, P.O. Box – 530 Maadi, Cairo, Egypt.

Abstract Um Bogma Formation is the most suitable lithological facies for uranium trapping adsorption, fixation, substitution and capturing as a result of the presence of clay and iron minerals in addition to the presence of the organic matter. The Lower Carboniferous Middle member of Um Bogma Formation at Wadi El Kharig composed mainly of marl and interbedded dolostone with pockets of gibbsite and marly gibbsite. The organic carbon (related to the presence of organic matter) reaches 2.31%, 6.39% and 1.36% in the marly gibbsite, black gibbsite and marl, respectively. The black gibbsite and marly gibbsite have high concentrations of some metals such as Zn, Cu, Ba and Ni than that in the marl. New detection of high radioactive anomalies were recorded at Wadi El Kharig in the marly gibbsite, black gibbsite and marl of the Middle member of Um Bogma Formation with an average of U-content reaches 342, 726.3 and 229 ppm, respectively. Metatorbernite, carnotite and autunite are the main secondary uranium minerals recorded in the radioactive facies. Also, new occurrences of gold were recorded at Wadi El Kharig in the marl (1.2 ppm) and its interbedded dolostone (1.4 ppm) of the Middle member of Um Bogma Formation. Carbonaceous material and/or organic matter in addition to the presence of iron oxides are playing important roles in concentrating of Au, U and some metals in the studied facies.

Key Words: Um Bogma, Carbonaceous material, organic matter

Date of Submission: 18-03-2020

Date of Acceptance: 03-04-2020

I. Introduction

Organic matters can reduce the mobility and precipitate the mobile trace and REEs elements these are highly mobile in oxidizing acidic water. This mobility is reduced by organic matter (Levinson 1980). Adams and Weaver (1958) and Adams et al. (1959), concluded that the distribution of uranium and thorium in sedimentary rocks are largely determined by the oxidation and leaching of uranium during weathering. The chemical and biochemical interactions affect the distribution patterns of uranium, thorium and their decay products. In the oxidized zone near-surface environment, uranium and thorium may be mobilized, but in different ways. Thorium is largely transported in insoluble resistant minerals or is adsorbed on the surface of clay mineral particles. While, uranium ions may either move in solution as a complex ion, or like thorium, move as adsorbed or in detrital phase. Uranium compounds are soluble under normal oxidizing conditions (Langmuir 1978). The oxidation process may be due to the action of the circulation of the ground meteoric water.

Um Bogma Formation is the most suitable lithological facies for uranium trapping adsorption, fixation, substitution and capturing as a result of the presence of clay and iron minerals in addition to the presence of the organic matter. Dabour and Mahdy (1988) recorded that uranium in the west central Sinai Carboniferous rocks exist in the hexavalent state and the secondary uranium minerals may represent the oxidation products of the pre-existing uranium minerals of the basement rocks.

The Paleozoic sediments were classified into Lower Sandstone Series, Middle Carbonate Series, and Upper Sandstone Series, (Barron 1907). Ball (1916) mapped the area. The Carboniferous age was assigned by (Issawi and Jux 1982). The Lower Sandstone Series were subdivided by Soliman and Abu El Fetouh (1969) into Sarabit El Khadim, Abu Hamata and Adedia Formations.

Weissbrod (1969) applied the term Um Bogma Formation to the Middle Carbonate Series, which was adopted by (Soliman and Fetouh 1969; Said 1971; El Shazly et al. 1974; Kora 1984; El Agami 1996 and Al Shami 2003). Omara and Conil (1965) classified the Um Bogma Formation into lower dolomitic member, middle dolomitic limestone member and upper dolomitic member, which was adopted by (Weissbrod 1969; Kora 1984; El Sharkawy et al. 1990; Mansour 1994), with some difference in detail. Also, the upper sandstone Series classified by Soliman and Abu El Fetouh (1969) into; El-Hashash, Magharet El-Maiah and Abu Zarab Formations.

The present study sheds the light on the geology, chemistry, radioactivity and mineralogy of the anomalous facies in the El Kharig area. Also, the work aims to investigate the different factors controlling in the gold, uranium and some base metals in the Lower Carboniferous marl in Wadi El Kharig area.

II. Geologic Setting

Wadi El Kharig area is covered by rock exposures ranging from Precambrian to Paleozoic age (Fig. 1). Precambrian igneous rocks are unconformably overlies by a thick Paleozoic sequences (Fig. 2A). The Precambrian comprises gneiss, schist, quartzdiorite and granite rocks. The Paleozoic rocks at Wadi El Kharig area comprise seven formations from base to top Sarabit El Khadim, Abu Hamata, Adedia, Um Bogma, El Hashash, Magharet El Maiah and Abu Zarab formations.

Sarabit El Khadim Formation

It unconformably overlies the basement rocks in the studied area. It composed mainly of cross-bedded sandstone (Fig. 2B) with conglomerate and pebbly sandstones (Fig. 2C) layer alternating with the sandstone in most localities that possess pinkish to brownish color.

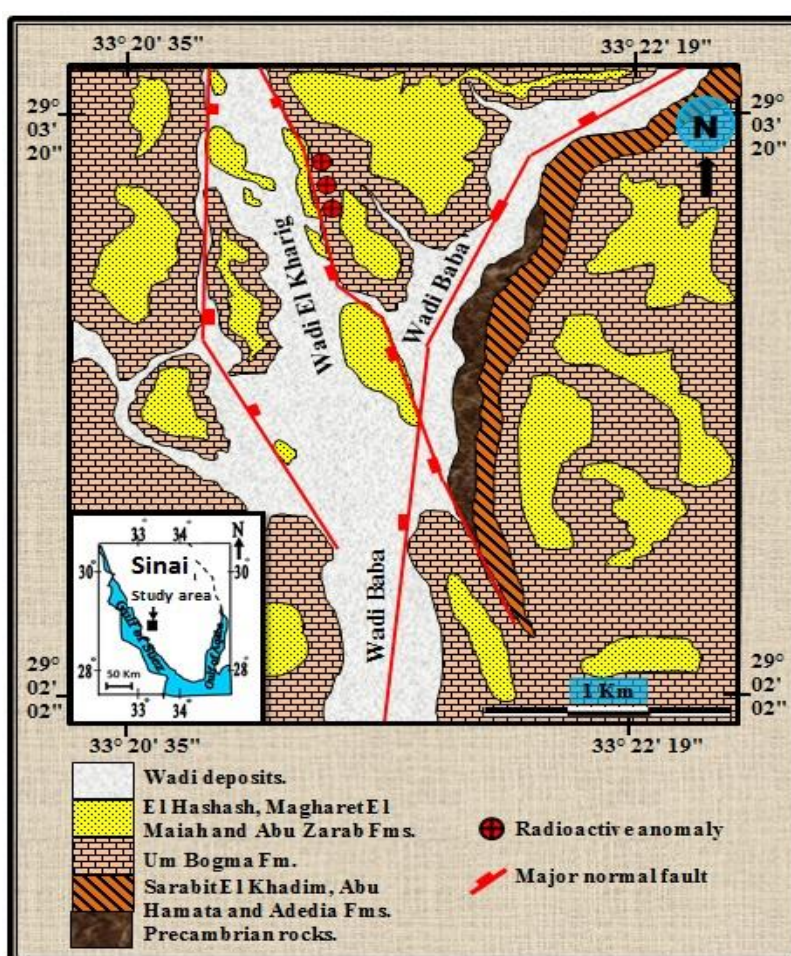


Fig. 1: Geological map of Wadi El Kharig area.

Abu Hamata Formation

It conformably overlies and underlies Sarabit El Khadim and Adedia Formations., respectively. It consists mainly of two members, the lower member is characterized by reddish color and composed of sandstone, siltstone and shale, while the upper member has greenish color which can be used as a marker horizon in the field and composed of fissile greenish shale, siltstone and very fine-grained sandstone.

Adedia Formation

The lower contact of Adedia Formation is well defined, but the upper is highly ferruginated. It consists of sandstone, very thickly bedded, fine grained, yellow, red and white incolor. These sandstones were used as building stones for the "ancient Egyptian Temple" at Gabal Sarabit El Khadim, near the study area.

Um Bogma Formation

Bogma Formation unconformably overlies Adediya Formation and unconformably underlies El Hashash Formation. The Lower member of Um Bogma Formation is represented by ferruginous siltstone with Mn-Fe lenses (Fig. 2D). The Middle member (Yellow bed) is represented mainly by yellow marl interbedded with dolostone (Fig. 2E). The Upper member is represented by dolostone interbedded with siltstone and claystone. Um Bogma formation is characterized by dominance of black organic matter filling the fissures. Marl of the middle member has gypsum (Fig. 2F), secondary copper minerals, organic matters and black gibbsite are recorded as veins and pockets (Fig. 3A). Gibbsite was recorded mainly in the Lower Carboniferous marl intercalated with dolostone in the middle member of the Um Bogma Formation. The main laterite mineral in the studied area is the gibbsite (El Aassy et al. 2000). Generally, gibbsite characterized by a high content of organic matter and occur in the form of discordant veins, pockets and lenses.

El Hashash Formation

It consists of brownish, cross-laminated sandstones, intercalated with thin beds of shale and siltstone (Fig. 3B). Ripple marks, trough and tabular planar cross stratification are observed in this formation.

Magharet El Maiah Formation

It consists of carbonaceous shale, sandstone, kaolin, and claystone (Fig. 3B). There is a lateral variation in the lithology of this formation, i.e., the kaolin beds change laterally into carbonaceous shale in two horizons. Exploratory old mines for kaolin and coal were excavated parallel to the formation. It can be easily identified in the field through its distinctive physical characteristics.

Abu Zarab Formation

It consists of white semi-friable sandstones with siltstone and shale (Fig. 3B), where some sandstone beds of this formation wedge out.

Generally, Um Bogma, El Hashash, Magharet El-Maiah and Abu Zarab are only the exposed Formations in Wadi El Kharig (Fig. 1).

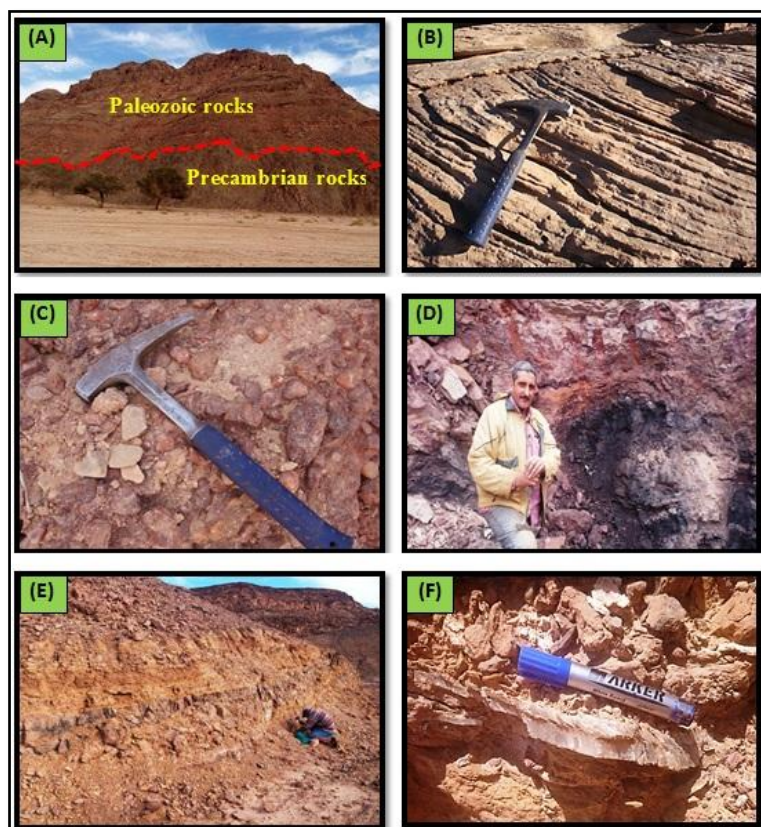


Fig. 2: Wadi El Kharig area; (A) Precambrian unconformably overlies by Paleozoic sequences, (B) Cross-bedded sandstone, Sarabit El Khadim Fm., (C) Conglomerate and pebbly sandstones, Sarabit El Khadim Fm., (D) Mn-Fe lens in the ferruginous siltstone, Lower member of Um Bogma Fm., (E) Yellow marl interbedded with dolostone, Middle member of Um Bogma Fm., (F) Gypsum veins in the marl, Middle member of Um Bogma Fm..

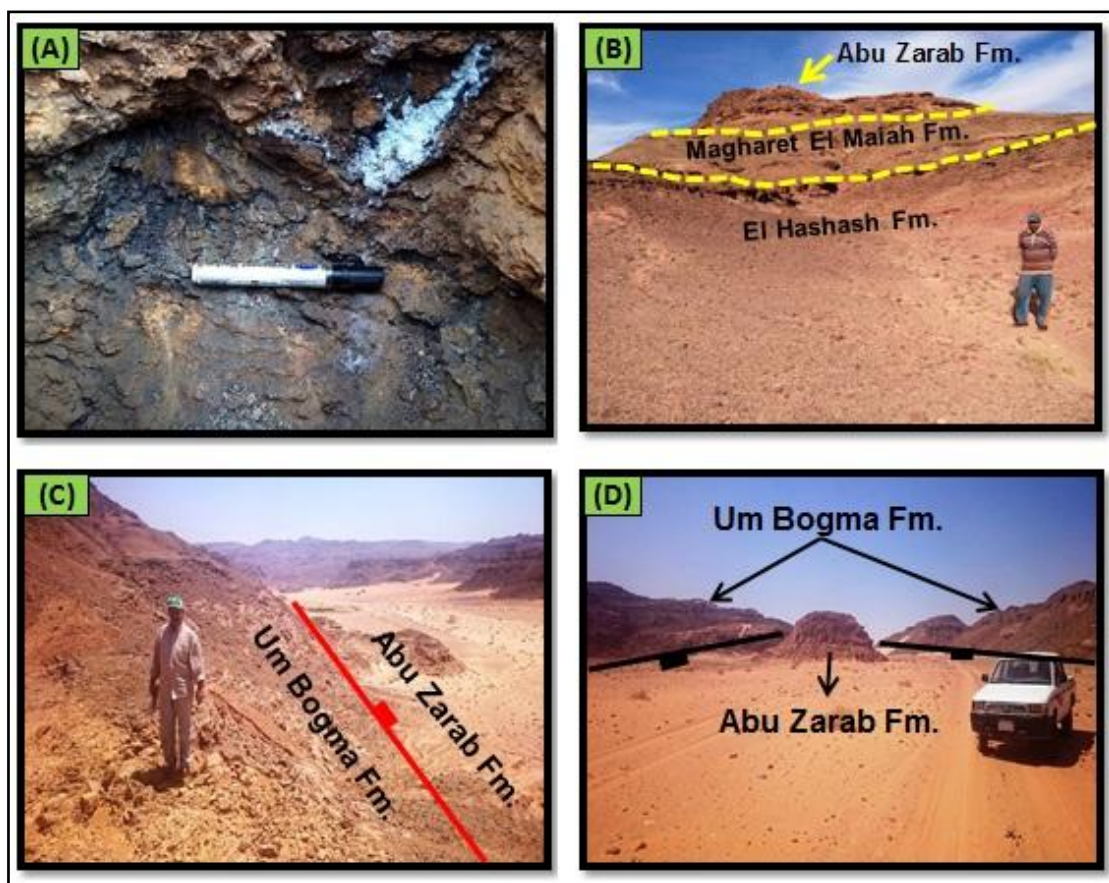


Fig. 3: Wadi El Kharig area; (A) Pocket of secondary copper minerals, organic matters and black gibbsite in the marl, Middle member of Um Bogma Fm., (B) El Hashash, Magharet El Maiah and Abu Zarab fms., (C) Normal fault, (D) Graben faults.

The Paleozoic rocks of the southwestern Sinai were subjected to several faulting systems that vary in throw from few centimeters to hundreds of meters. Also, they vary in trends where the most common ones are NW, NE, NS and EW. Alshami (2017) recorded that the NW-trending faults controlled the high U-concentration at Wadi Nasib, Talet Selim, Moreid and Abu Hamata, whereas the NE-trending faults controlled the U-concentrations at Baba while the EW-trending faults controlled the U-concentration at El Sahu. Wadi El Kharig is located within the down-thrown block of the Wadi Baba normal fault (Fig. 1) and affected by a number of normal faults (Fig. 3C) constituting a graben fault (Fig. 3D) trending NW.

III. Materials and Methods

Field radiometric measurements were performed using a handheld gamma-ray spectrometer (Model Rs-230 BGO Super-Spec, Radiation Detection Systems AB, Backehagen, Sweden) for the determination of eU (ppm), eTh (ppm) and K%. The frequency for acquiring radiometric measurements was set every 30 s. Mention the spacing of measurements in field (is constant spacing on grid pattern or random)

The chemical concentrations of the major oxides were determined using Shapiro and Branock methods (1962). Inductively coupled plasma optical emission spectrometry (720 ICP-OES Agilent Technologies, Santa Clara, CA, USA) was used for measuring uranium, trace and rare earth elements (REEs). These analyses were carried out at the Central Laboratory Sector of the Egyptian Mineral Resources Authority (EMRA). Mineral samples (crushed and sieved to 200 Mesh) were digested in teflon crucibles using 0.5 g of grinded sample with 3 mL of perchloric acid, 5 mL of nitric acid and 15 mL of hydrofluoric acid: the mixture was covered with a glass lens and heated for 3 hours till complete digestion; in a second step the glass lens was removed to evaporate silica tetrafluoride till complete evaporation. Five mL of concentrated HCl were added to dissolve the solid residue; after drying under heating the solid was completely dissolved with 50 mL HCl aqueous solution (1:1 w/w); the volume was adjusted to 100 mL with distilled water and the concentration of metal ions analyzed by ICP-AES (720 ICP-OES, Agilent Technologies, Santa Clara, CA, USA).

The determination of gold content required a specific procedure; fire assay analysis was carried out at EMRA. Fifty g of samples (crushed and sieved to 200 Mesh) were fired in the presence of alkali fusion agents.

More specifically the grinded sample was added to a mixture of litharge, borax, sodium carbonate, flour, silica and silver in a ceramic crucible. The mixture was melt at 1000 °C for 90 min; this step was followed by the cupellation of lead/gold/silver alloy at 900 °C for 60 min. The resulting alloy (Ag/Au) was then dissolved with concentrated nitric acid and aqua regain under heating to dissolve gold; the solution was further analyzed by atomic absorption spectrometry (using a Savant AA spectrometer, GBC Scientific Instruments, Braeside, Australia).

The mineralogical composition of the samples required a preliminary conditioning of the samples. 3 to 5 kg of selected samples were crushed and sieved to collect the fraction 0.074 mm-0.5 mm, 35-200 Mesh). The sieved fraction was submitted to two separation steps: (a) densitometry separation using bromoform (Sp.G.: 2.85-2.89)(Quinif et al.2006)and (b) magnetic separation using a Frantz Isodynamic Magnetic Separator (S.G. Frantz Co., Inc, Tully town, PA, USA). For magnetic separation, the side slope was set at 5° and the forward slope at 20° under and amperage of 0.5 A(Flinter 1959). Separated fractions were picked using binocular microscope (Meiji, Japan), and investigated with Environmental Scanning Electron Microscope ESEM (XL30-ESEM, Philips, FEI, Thermo Fisher Scientific, Hillsboro, OR, USA) associated with attached energy dispersive X-ray spectrometer (EDX) unit, was operated at 25–30 kV accelerating voltage, 1–2mm beam diameter and 60–120 s counting time. Polished sections were specifically analyzed using a Quanta FEG200, FEI-France, Thermo Fisher Scientific, Merignac, France) coupled with an Oxford Inca 350 EDX microanalyzer (Oxford Instruments France, Saclay, France) at the C2MA at IMT – Mines Ales.

IV. Results and Discussions

4.1. Geochemistry

The anomalous samples of Um Bogma Formation(marly gibbsite,black gibbsite andmarl) were chemically analyzed to determine their major oxides (%), trace (ppm) and rare earth elements content (ppm) (Tabs. 1).

Table 1: Chemical analysis of the studied anomaloussamples,Wadi El Kharig area.

Formation	Middle Um Bogma					
Rock type	Marly gibbsite		Black gibbsite		Marl	
Sample No.	4	6	1	3	8	10
Major oxides in %						
SiO ₂	38.63	35.35	20.1	19.93	47.18	45.5
Al ₂ O ₃	18.45	19.43	36.65	37.47	16.45	15.71
TiO ₂	0.7	0.64	0.18	0.21	0.7	0.42
Fe ₂ O ₃ ¹	16.41	15.92	18.56	17.32	11.33	12.53
MgO	3.92	2.3	2.04	1.10	3.45	4.61
CaO	4.1	5.7	2.17	3.24	4.32	4.17
Na ₂ O	5.3	3.36	0.73	0.63	2.77	2.48
K ₂ O	1.34	2.0	0.72	0.91	1.7	1.47
MnO	3.1	4.3	3.08	2.08	2.19	3.44
P ₂ O ₅	0.6	0.15	0.11	0.13	0.1	0.12
CO ₂	2.1	2.7	1.1	1.01	4.9	5.3
S	1.0	0.8	1.6	1.5	0.9	0.7
C	2.17	2.31	3.64	6.39	1.07	1.36
L.O.I.	2.1	5.01	8.4	8.06	3.0	2.07
Total	99.92	99.95	99.08	99.98	99.43	99.88

Table 1: Cont.

Fm.	Middle Um Bogma Fm.											
Rock Type	Marly gibbsite				Black gibbsite				Marl			
S.No	4	5	6	7	1	2	3	12	8	9	10	11
Trace elements in ppm												
Cu	8342	9298	9018	9102	4180	4039	4049	4050	503	419	335	475
Ni	270	242	243	254	4571	4204	4500	4269	284	281	300	267
Zn	2047	2118	2092	2145	15827	15371	15466	15286	2548	2503	2416	2554
Zr	980	871	905	962	1000	912	895	923	918	751	809	917
Ga	44	17	55	53	4	2	31	82	66	11	223	65
Sr	573	495	501	537	748	713	704	714	387	325	339	389
Y	407	347	373	410	182	160	159	162	93	72	79	74
Rb	285	218	248	285	1	2	4	2	21	28	18	47
V	1466	935	1176	1447	523	540	528	517	611	607	563	565
Nb	57	65	86	70	51	42	40	42	30	25	24	26
Pb	395	271	264	268	508	478	487	491	458	430	441	546
Ba	3778	3933	4008	3924	6722	1868	6735	5825	2147	2165	1889	2180
U	413	296	317	-	735	615	829	-	235	211	241	-

Table 1: Cont.

Fm.	Middle Um Bogma Fm.		
Rock type	Marly gibbsite	Black gibbsite	Marl
S.No	6	3	8
Rare earth elements in ppm			
La	37	74	45
Ce	70	126	142
Dy	5.1	10	13
Er	4.5	10.5	6.4
Eu	1.9	6.1	3.3
Gd	10.7	21.1	20
Ho	N.D	N.D	N.D
Lu	1.9	7.2	2
Nd	35	63	50
Pr	16	27	14
Sm	5.1	13.1	8
Tb	2.5	7.8	4.1
Tm	N.D	N.D	N.D
Y	25	55	60
Yb	3.2	91	5.1
ΣREEs	200.4	514.8	382.9
La/Y	1.5	1.3	0.8

Table 1 reveals that the anomalous samples have high concentrations of iron oxides ($Fe_2O_3^5$) reaches 19.41%, 18.56% and 12.53% in the marly gibbsite, black gibbsite and marl, respectively. The organic carbon (related to the presence of organic matter) reaches 2.31%, 6.39% and 1.36% in the marly gibbsite, black gibbsite and marl, respectively.

The selected anomalous samples of the marl has high concentrations of Zn, Ba, Zr, V, Pb, Cu, Sr, Ni and Ga in which reaches 2554 ppm, 2180 ppm, 918 ppm, 611 ppm, 546 ppm, 503 ppm, 389 ppm, 300 ppm and 223 ppm respectively. The black gibbsite show high concentration in Zn, Ba, Ni, Cu, Zr, Sr, V, Pb and Y reaches 15827 ppm, 6735 ppm, 4571 ppm, 4180 ppm, 1000 ppm, 748 ppm, 540 ppm, 508 ppm and 182 ppm respectively. Also, the marly gibbsite reflect high concentration in Cu, Ba, Zn, V, Zr, Sr, Y, Pb, Rb and Ni reaches 9298 ppm, 4008 ppm, 2145 ppm, 1466 ppm, 980 ppm, 573 ppm, 410 ppm, 395 ppm, 285 ppm and 270 ppm respectively.

The trace elements measurements in this study normalized to the North American Composite Shale (NASC, Gromet et al. 1984). The studied facies show high enrichment in Y and in all of the compared heavy metals especially Ni, except black gibbsite and marl samples show depletion in Rb (Fig. 4A).

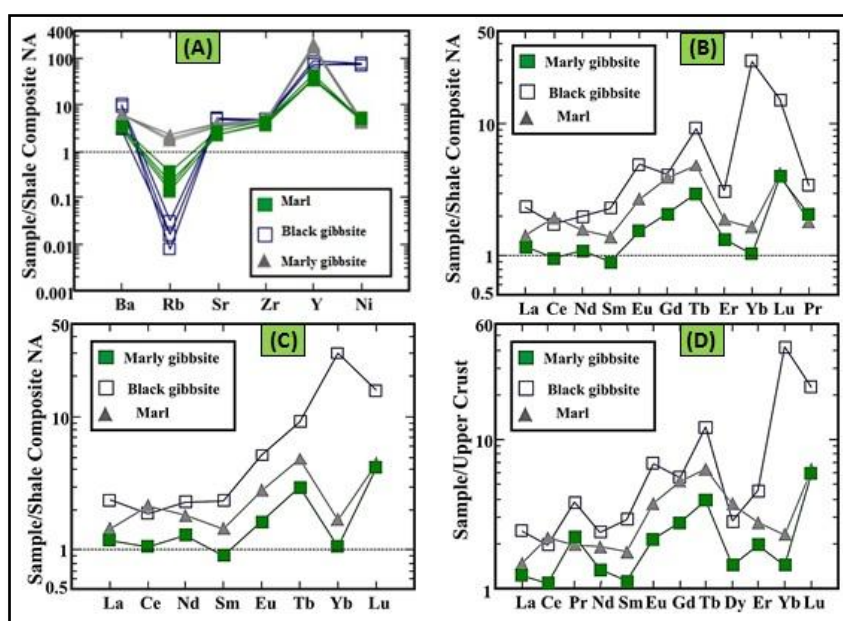


Fig. 4: Wadi El Kharig area; (A) Average trace elements concentrations in the studied facies as normalized to the NASC (Gromet et al. 1984), (B) Normalized REEs according to NASC (Haskin et al. 1968), (C) Normalized REEs according to NASC (Gromet et al. 1984), (D) Normalized REEs to UCC (Taylor and McLennan 1981).

Adsorption process and activity of organic matter plays a role in precipitation of trace elements. The black gibbsite and marly gibbsite samples have high concentrations of some metals such as Zn, Cu, Ba and Ni than that in the marl samples; these may be attributed to the high content of organic matter and iron oxides in the black gibbsite and marly gibbsite samples. Mira et al. (2006) concluded that organic matter play a major role in absorption and precipitation of uranium, some metals such as Zn, Pb, Ni, Cu, Mn, Fe, P and Sr and some rare earth elements.

The La/Y ratio as geochemical parameter used to interpret the pH conditions of depositional environment of the different facies in the middle member of Um Bogma Formation. Values > 1 and < 1 for La/Y ratio is related to alkaline and acidic environment, respectively (Crinci and Jurkovic 1990; Maksimovic and Pantó 1996). Value of La/Y ratio < 1 in the marl while La/Y ratio > 1 in the gibbsite and marly gibbsite provide reasons to believe that gibbsite and gibbsitic marl have alkali condition due to the high concentration of organic matter while marl has acidic conditions (due to the dissolved CO_2) were prevailed in the meteoric percolating waters (Fernandez-Caliani and Cantano 2010).

Therefore, it can be concluded that trace and rare earth elements were likely leached from the acidic environments and concentrated in the alkaline zone under reducing conditions. Though, trace and REEs in black gibbsite are higher than other studied facies.

REEs patterns of the analyzed facies are demonstrated, as normalized to north American Shale Composite (NASC) abundances (Haskin et al. 1968, Gormet et al. 1984) (Figs. 4B&C). According to the normalization patterns, there is enrichment of the all rare earth elements of different facies normalized to NASC especially Yb and Lu of the black gibbsite and except Sm show slightly depletion in the marly gibbsite.

Also, The REEs measurements of the different anomalous facies normalized to the upper continental crust (UCC) of Taylor and McLennan 1981 (Fig. 4D). According to the normalization pattern, there is enrichment of the all rare earth elements of different facies normalized to UCC especially Yb and Lu of the black gibbsite.

Chemical correlations:-

Concentration of uranium controlled by the percent's of carbon and iron oxides present in the different facies this indicated by the positive correlation of uranium with carbon (Fig. 5A) (organic matter) and iron oxides (Fig. 5B). U is more adsorbed on gibbsite than on clay minerals this can be concluded from its positive correlation with Al_2O_3 (Fig 5C) and negative correlation with SiO_2 (Fig. 5D). While the correlation of uranium with REEs (Fig. 5E) and of carbon with REEs (Fig. 5F) gives undefined relations.

4.2. Radioactivity

The radioactivity was recorded in several units in Sinai. The most notable one were recorded in the Paleozoic rocks, especially in Um Bogma Formation. It is the most important formation in the Paleozoic succession from the radioactivity and mineralizations points of view. Most of the radioactive anomalies are concentrated in definite stratigraphic horizon among them; the most significant uranium occurrences are located in the Middle member of Um Bogma Formation in the study area.

The radiometric investigations of the different facies at Wadi El Kharig lead to record three high radioactive anomalies (first recorded) in the marly gibbsite, black gibbsite and marl of the Middle member of Um Bogma Formation (Table 2). The anomalous marly gibbsite show eU-contents range between 320 ppm and 460 ppm with an average of 372 ppm. The highest eU-contents concentrated in the black gibbsite, it ranges between 1030 ppm and 911 ppm with an average of 980.7 ppm. The eU-contents in the marl vary from 230 ppm to 280 ppm with an average of 255.7 ppm.

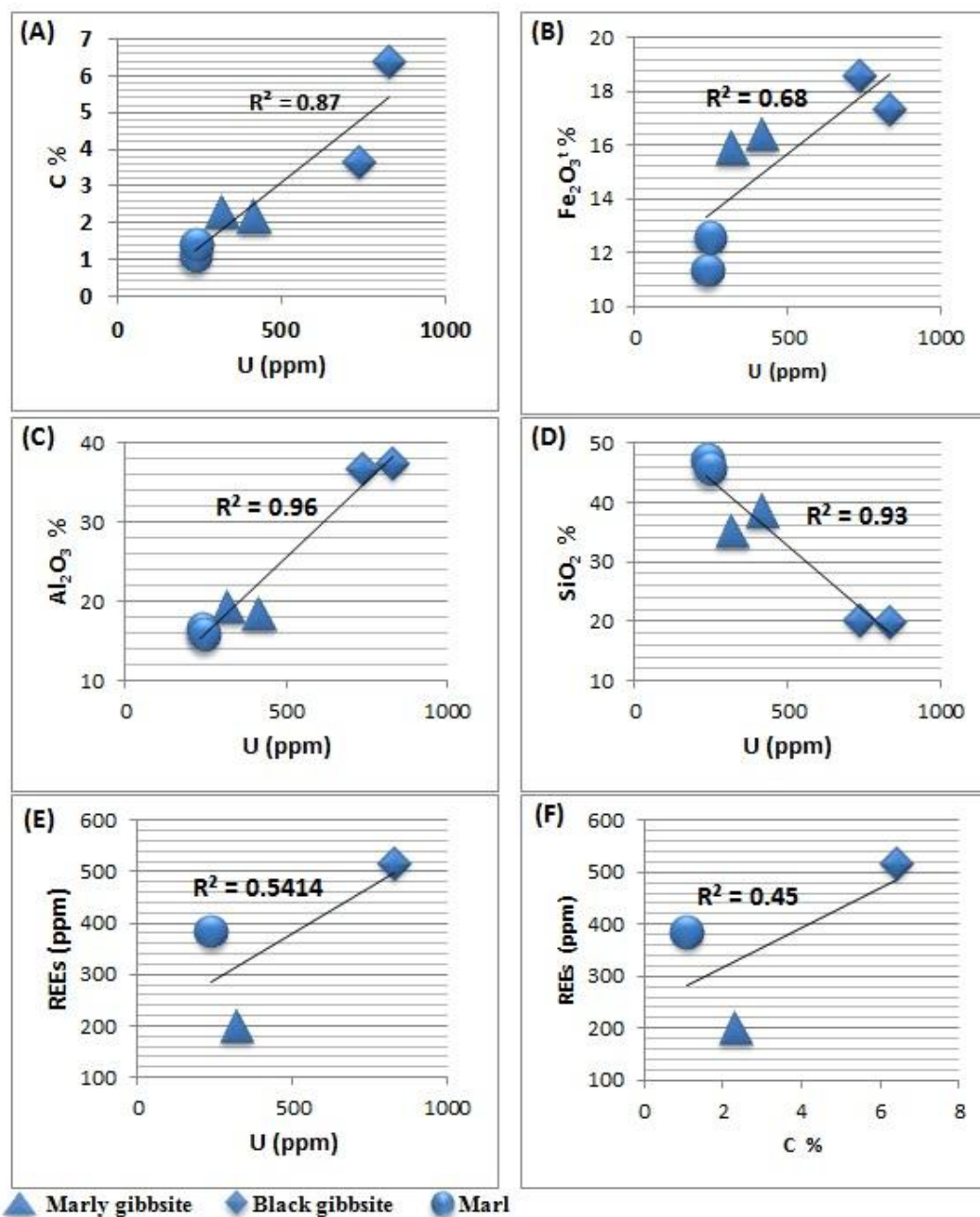


Fig. 5: Some chemical correlations, Wadi El Kharig area.

Table 2: Radiometric and chemical measurements of the anomalous facies, Wadi El Kharig area.

Age	Fm.	Rock unite	Sample No.	eU (ppm)	Uc (ppm) Chemically	eTh (ppm)	eU/eTh	Uc/eU
Lower Carboniferous	Middle Um Bogma	Marly gibbsite	4	460	413	69	6.7	0.9
			5	320	296	71	4.5	0.93
			6	336	317	43	7.8	0.94
			Max.	460	413	71	7.8	0.94
			Min.	320	296	43	4.5	0.9
			Average	372	342	61	6.3	0.92
		Black gibbsite	1	1030	735	87	11.8	0.71
			2	911	615	62	14.7	0.68
			3	1001	829	77	13	0.83
			Max.	1030	829	87	14.7	0.83
			Min.	911	615	62	11.8	0.68
			Average	980.7	726.3	75.3	13.2	0.74

	8	280	235	49	5.7	0.84
Marl	9	230	211	56	4.1	0.92
	10	257	241	73	3.5	0.94
Max.		280	241	73	5.7	0.94
Min.		230	211	49	3.5	0.84
Average		255.7	229	59.3	4.4	0.90

The eU/eTh ratio is a very important index for determining uranium migration in or out. The Clark value for eU/eTh in the sedimentary rocks is equal unity (Clark et al. 1966). The eU/eTh ratio of the studied anomalous facies varies between 13.2 to 4.4 times Clark value, these reveals that the studied anomalous facies have migration in (leaching) of uranium. Black gibbsite has the highest eU/eTh (13.2) (Table 2) this may attributed to their highest contents of organic matter and iron oxides reaches 6.39 % and 18.56 % (Tab. 1), respectively, which playing an important factors in capture of uranium.

Hansink (1976) introduced the D-factor, which defines the equilibrium factor as the ratio between the chemically determined uranium chemically (Uc) and the radiometrically measured uranium (eU). If the factor was more or less than 1.0, it indicates disequilibrium state which, could be attributed to the addition or removal of U.

Hambleton-Jones and Andersen (1984) introduced the ratio chemical U_3O_8 / Spectrometric eU_3O_8 as a measure of the disequilibrium in the U deposit, in which:

- Values > 1 = Positive disequilibrium. Uranium has been recently deposited giving a low equivalent grade and a high chemical assay. This implies that uranium is young and the ^{226}Ra has had insufficient time to attain secular equilibrium.

- Values equal to 1 = Secular equilibrium.

- Values < 1 = Negative disequilibrium. Uranium has been leached, leaving a proportion of unsupported ^{226}Ra behind. This will result in a high equivalent grade and a low chemical assay.

Chemical measurements of the U-content of the anomalous facies in the study area are lower than those of field radiometric measurements (eU) (Table 2), this indicates that all the studied anomalous facies are in negative disequilibrium state due to removal of uranium. This means that some of uranium in these rocks has been removed leaving the daughter products behind, hence the level of radioactivity is higher than would be expected for the amount of uranium present.

Organic matter has long been known to be associated with many types of mineral deposits, especially certain types of uranium deposits. Because reduced uranium species have a much smaller solubility than oxidized uranium species and because of the strong association of organic matter (a powerful reductant) with many uranium ores, reduction has long been considered to be the precipitation mechanism for many types of uranium deposits (Charles S. Spirakis 1996). He also noticed that the strong association of organic matter with uranium deposits in sedimentary rocks and the change in the character of the deposits from physical to chemical concentrations concomitant with the change in the oxidation state of the atmosphere indicate that reduction is the most important chemical process involving organic matter in the genesis of uranium deposits. This explains the high concentration of uranium contents in black gibbsite (the highest content of organic matter) than the other anomalous facies.

So, according to the organic matter enrichment in the studied samples, we can conclude that uranium may precipitate under reduction conditions. Generally, The high values of U-contents in the studied samples could be attributed to the leaching concept; in which, the uranium has been leached from other surrounding rocks, transported by means of circulating water and finally captured and deposited by the organic matter in addition to the iron oxides present in the studied facies.

4.3. Mineralogical Investigations

4.3.1. Gold (Au)

Sallam et al. (2014) recorded minerals bearing Ag and Au namely uytenbogaardtite and furutobeite in the lower member of Um Bogma Formation at El Sheikh Soliman Area. Alshami (2018) detected gold in Um Bogma Formation at Allouga quarry with concentration reaches 9.7 ppm.

Carbonaceous material and/or organic matter is thought to be a key reductant contributing to the formation of large Au deposits (Aileen Mirasol-Robert et al. 2017). Au deposits are commonly associated with carbonaceous sediments suggesting carbon materials may be an important factor in Au mineralization processes. Many gold deposits and indeed Au-bearing fluids occur in Proterozoic terrains with predominantly carbonaceous shale or sedimentary host rocks (Goldfarb et al. 2001).

Organic matter may potentially share a large number of intimate relationships with Au during its transportation, accumulation or deposition (e.g., redox or catalytic reactions, solubility changing complexations,

co-transportation in hydrothermal fluids or co-accumulation in porous rocks; (Gize 2000; Greenwood et al. 2013).

Four samples from the anomalous radioactive gibbsite, marly gibbsite, marl and its intercalated dolostone of the middle member of Um Bogma Formations were analyzed for measuring their gold contents. Anomalous contents of gold at Wadi El Kharig are first recorded in the studied lithofacies bulk samples of the marl (reaches 1.2 ppm) and its intercalated dolostone (reaches 1.4 ppm) of the middle member of Um Bogma Formation, while the other two facies show negative gold content. The gold present in fine-grain size and smooth-edge particles (Fig. 6A).

The identified gold may be concentrated by the carbonaceous material and/or organic matter present in the marl and dolostone during means of transportation of Au from the surrounding hydrothermal deposits as its high resistance to both chemical and physical weathering and its high specific gravity. EDAX data carried out on the chosen spots within the polished sections show that the elements associated with gold includes Cu, S, Pb, P, Th, Y, Ni, Ba, Mn, Fe, Zn and As (Figs. 6, 7 & 8A).

ESEM investigations and XRD analysis of the studied anomalous samples indicated that, the most important U- and Th-minerals include metatorbernite, carnotite, autunite and uranorthorite, while U-bearing minerals represented by zircon. Chrysocolla and galena are found as base metals minerals and celestine is also detected. The present mineralogical study clarified the presence of secondary uranium minerals that may represent the oxidation products of the pre-existing uranium minerals in the surrounding basement rocks. The uranium may also be present in the lattice of the identified accessory minerals such as zircon and xenotime as detected by the mineralogical investigations.

4.3.2. U-minerals

Metatorbernite $Cu^{++}(UO_2)_2(PO_4)_2 \cdot 8H_2O$

It is a radioactive phosphate mineral, and is a dehydration pseudomorph of torbernite. Chemically, it is a copper uranyl phosphate and usually occurs in the form of green platy deposits. It can form by direct deposition from a supersaturated solution, which produces true crystalline metatorbernite. Metatorbernite present as unihedral flakes with a dark green colour (Figs. 8B & 9A).

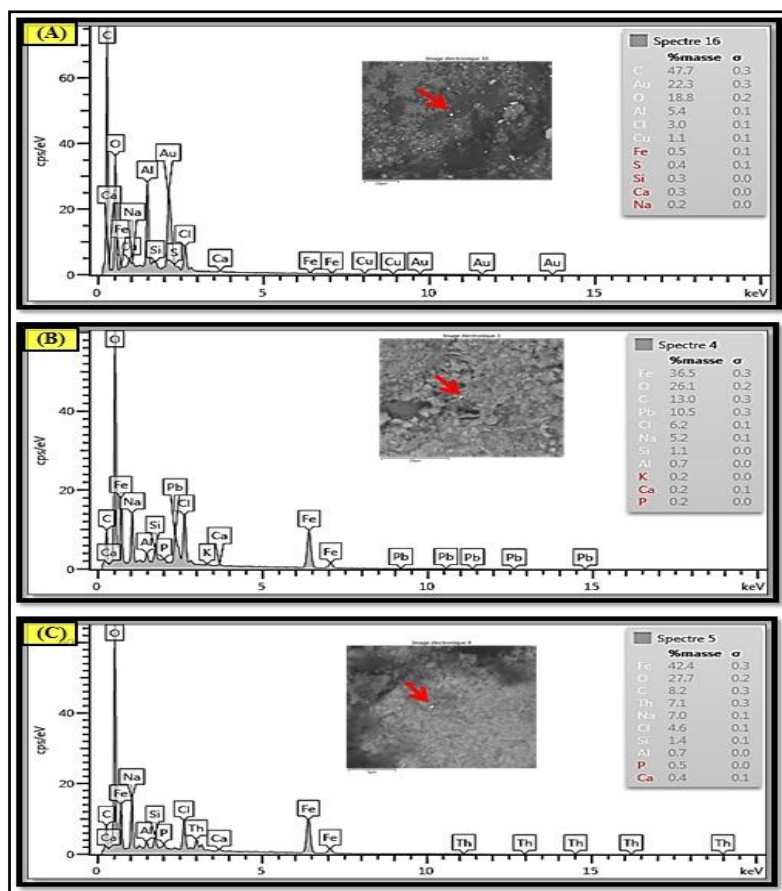


Fig. 6:EDX spectrum and BSE image showing: (A) Au, Cu & S, (B) Pb and (C) Th & Fe.

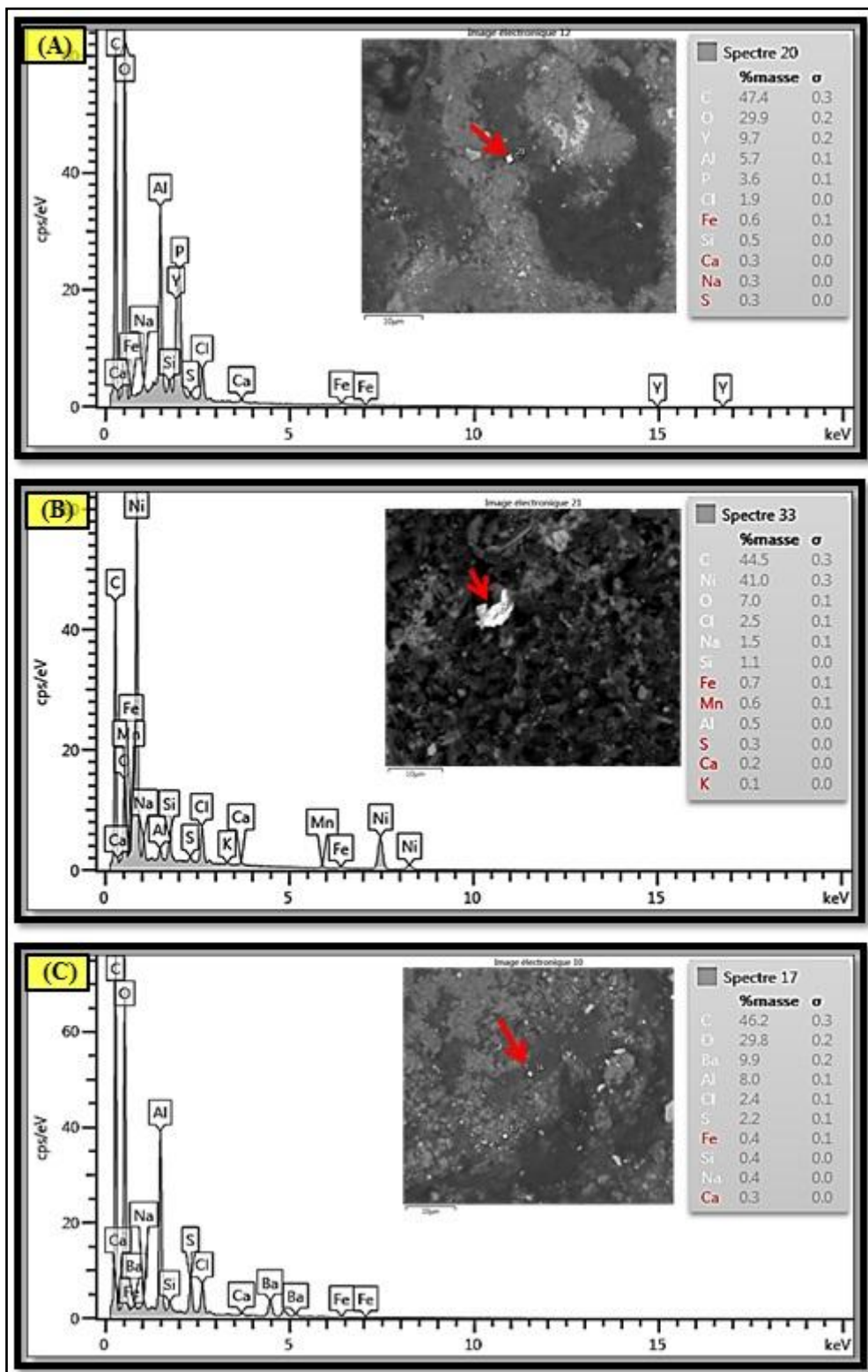


Fig. 7:EDX spectrum and BSE image showing: (A) Y & P, (B) Ni and (C) Ba.

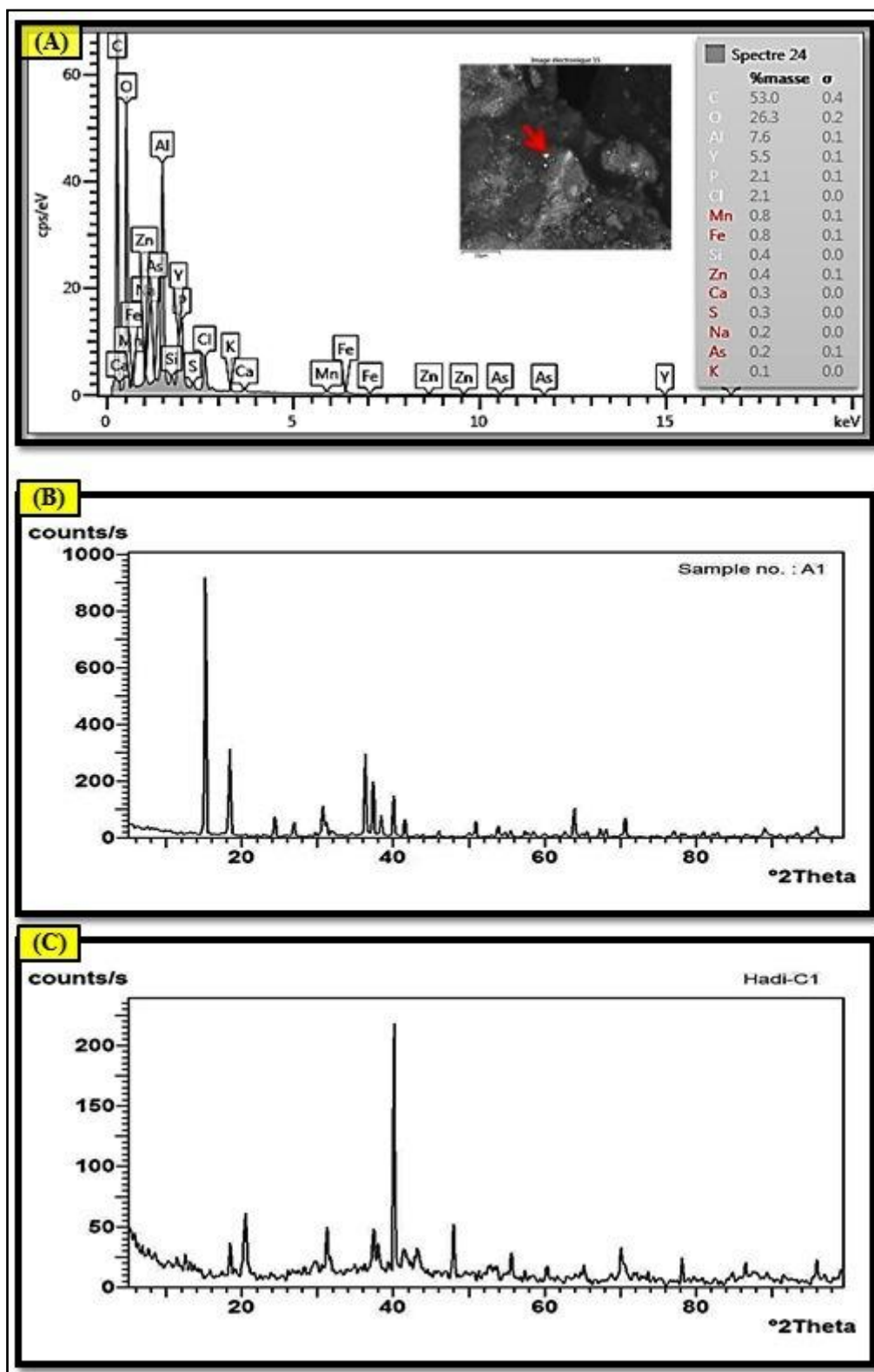


Fig. 8: (A) EDX spectrum and BSE image showing: Zn & As, (B) X-ray diffraction pattern of metatorbernite, (C) Fig. 10: X-ray diffraction pattern of carnotite.

Carnotite $K_2(UO_2)_2(VO_4)_2 \cdot 3H_2O$

It is a secondary vanadium and uranium mineral usually found in sedimentary rocks in arid climates. Carnotite forms subhedral crystals with a lemon-yellow colour (Fig.8C & 9B).

Autunite $Ca(UO_2)_2(PO_4)_2 \cdot 10-12H_2O$

It is hydrated calcium uranyl phosphate. Autunite can lose water and convert to a different mineral called meta-autunite-I of the meta-autunite/meta-torbernite group of minerals and with heating can produce a meta-autunite-II mineral (<https://en.wikipedia.org/wiki/Autunite>). This mineral is to some extent highly speckled in the oxidation zones of most uranium deposits (Cesbron et al. 1993). Autunite crystals present as soft aggregates and of bright yellow colour (Fig.9C).

4.3.3. Th- and U-minerals

Uranothorite $(Th,U)SiO_4$

It occurs as yellow to yellowish brown unihedral crystals (Fig.9D). It is uranium-rich variety of thorite and contains uranium up to 12 % while ThO_2 range from 49 to 75 %, also there are other elements commonly present in minor amounts such as Ca, Mg, Fe, alkalis, Ce earths, P, Ta, Ti, Zr, Sn and Al (Heinrich 1958).

4.3.4. Associated minerals

Zircon $ZrSiO_4$

Form subhedral yellowish to reddish brown colour (Fig. 9E). Because of their uranium and thorium content, some zircons undergo metamictization. Connected to internal radiation damage, these processes partially disrupt the crystal structure and partly explain the highly variable properties of zircon. As zircon becomes more and more modified by internal radiation damage, the density decreases, the crystal structure is compromised, and the color changes.

Zircon has played an important role during the evolution of radiometric dating. Zircons contain trace amounts of uranium and thorium (from 10 ppm up to 1 wt%) and can be dated using several modern analytical techniques. Because zircons can survive geologic processes like erosion, transport, even high-grade metamorphism, they contain a rich and varied record of geological processes (<https://en.wikipedia.org/wiki/Zircon>).

4.3.5. Base metals minerals

Chrysocolla $(Cu,Al)_2H_2Si_2O_5(OH)_4 \cdot nH_2O$

It forms unihedral ball blue colour crystals (Fig. 9F). Chrysocolla is of secondary origin and forms in the oxidation zones of copper sulfide mineral deposits.

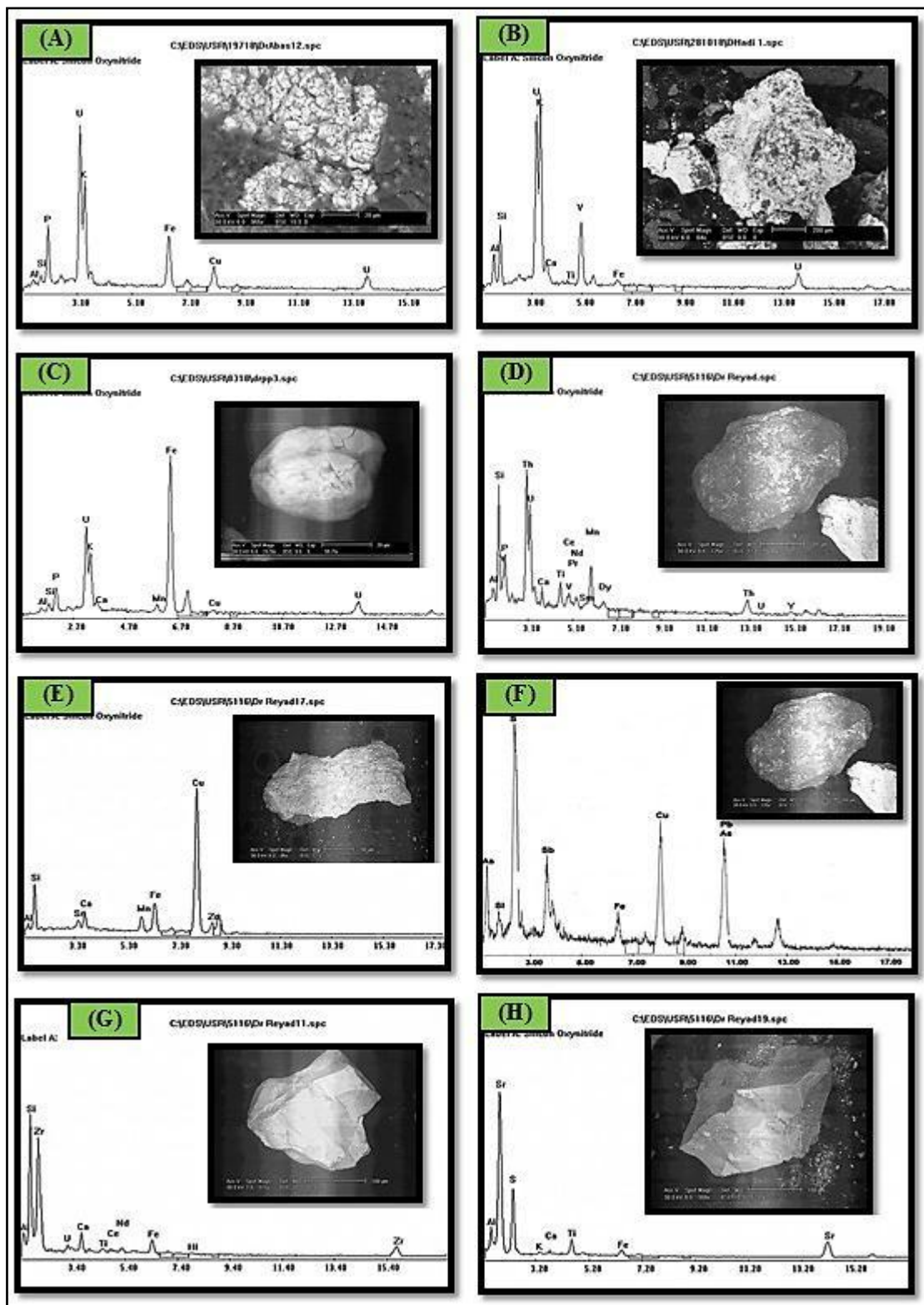


Fig. 9: EDX spectrum and BSE image of: (A) Metatorbernite, (B) Carnotite, (C) Autunite, (D) Uranothorite, (E) Zircon, (F) Chrysocolla, (G) Galena and (H)Celestine.

GalenaPbS

It is the natural mineral form of lead(II) sulfide. Galena typically forms in low-temperature sedimentary deposits. Galena found as unhedral crystals with lead-grey colour (Fig. 9G)

Celestine SrSO₄

It is mostly found in sedimentary rocks, often associated with the minerals gypsum, anhydrite, and halite. Celestine crystal has Colorless to light blue colour (Fig. 9H).

V. Conclusions

Adsorption process and activity of organic matter in addition to the presence of iron oxides plays important roles in precipitation of trace and rare earth elements and uranium. The black gibbsite and marly gibbsite samples have high concentrations of some metals such as Zn, Cu, Ba and Ni than that in the marl samples; these may be attributed to the high content of organic matter and iron oxides in the black gibbsite and marly gibbsite samples.

New detection of high radioactive anomalies were recorded at Wadi El Kharig in the marly gibbsite, black gibbsite and marl of the Middle member of Um Bogma Formation with an average of U-content reaches 342, 726.3 and 229 ppm, respectively. According to the organic matter enrichment in the studied samples, we can conclude that uranium may precipitate under reduction conditions. The high values of U-contents in the studied samples could be attributed to the leaching concept; in which, the uranium has been leached from other surrounding rocks, transported by means of circulating water and finally captured and deposited by the organic matter in addition to the iron oxides presents in the studied facies.

The most important U- and Th-minerals detected in the radioactive facies include metatorbernite, carnotite, autunite and uranothorite.

Also, new occurrences of gold were recorded at Wadi El Kharig in the marl (1.2 ppm) and its interbedded dolostone (1.4 ppm) of the Middle member of Um Bogma Formation. The identified gold may be concentrated by the carbonaceous material and/or organic matter present in the marl and dolostone during means of transportation of Au from the surrounding hydrothermal deposits as its high resistance to both chemical and physical weathering and its high specific gravity.

Acknowledgements

The author acknowledges the support of the Nuclear Materials Authority (NMA), Cairo, Egypt, for their kind field and laboratory facilities during the preparation of this work.

References

- [1]. Adams, JAS, Osmund K and Rogers JJW (1959) The geochemistry of thorium and uranium, *Physics and Chemistry of the Earth*. 3, pp298-343, Pergamon press, London.
- [2]. Aileen Mirasol-Robert, Hendrik Grotheer, Julien Bourdet, Alexandra Suvorova, Kliti Grice T. Campbell McCuaig, Paul F Greenwood (2017) Evidence and origin of different types of sedimentary organic matter from a Paleoproterozoic orogenic Au deposit. *Precambrian Research* 299, pp 319–338.
- [3]. Alshami AS (2003) Structural and lithologic control of uranium and copper mineralization in the Um Bogma environs, southwestern Sinai, Egypt. Ph.D. Thesis, Fac. of Sci., Mansoura Univ., Egypt, 205p.
- [4]. Alshami AS (2017) U-minerals and REE distribution, paragenesis and provenance of Um Bogma Formations, southwestern Sinai, Egypt. *Nuclear Sciences Scientific Journal*.
- [5]. Alshami AS (2018) Infra-Cambrian placer gold-uraniferous Paleozoic sediments, southwestern Sinai, Egypt. *Nuclear Sciences Scientific Journal*.
- [6]. Ball J (1916) *The Geography and Geology of West Central Sinai*, Egypt. Survey Dept., Cairo, 219p.
- [7]. Barron T (1907) *The topography and geology of the peninsula of Sinai (Western portion)*, Egypt. Surv. Dept., Cairo, 241 p.
- [8]. Cesbron A, Moreau P, Rapp MJ, Cheneau ML, Herry P, Bonneville F, Muller JY, Harrouseau JL and Bignon JD (1993) HLA-DPB and susceptibility to Hodgkin's disease. *Hum Immuno*, pp136: 51
- [9]. Clark SP, Peterman ZE and Heier KS (1966) Abundance of uranium, thorium and potassium. In: S.P. Clarke, Jr., (Editor), *Handbook of Physical Constants*, Geol. Soc. Am. Mem. 97, Section 24, pp521-541.
- [10]. Crinci J, Jurkovic I (1990) Rare earth elements in Triassic bauxites of Croatia
- [11]. Yugoslavia. In: *Travaux*. 19, pp 239–248.
- [12]. Charles S. Spirakis (1996) The roles of organic matter in the formation of uranium deposits in sedimentary rocks. *C.S. Spirakis / Ore Geology Reviews* 11, pp53-69.
- [13]. Dabbour GA and Mahdy, MA (1988) Mineralogical studies on the Carboniferous
- [14]. uraniumiferous sediments in west central Sinai, Egypt., 4 th Conf. Nuc. Sc. and appl., Cairo, Egypt, (p21-36), pp230-237.
- [15]. El Agami NL (1996) Geology and radioactivity studies on the Paleozoic rock units in Sinai Peninsula, Egypt; Ph.D. Thesis, Fac. Of Sc., Mansoura Univ.
- [16]. El Aassy IE, Fadia FY, Afifi SY and El Shamy AS (2000) Uranium in laterites, southwestern Sinai, Egypt; 1st seminar on Nuclear Raw Materials and their Technology, Cairo, Egypt, 1-3 Nov., pp1-20.
- [17]. El Sharkawi MA, El Aref MM and Abdel Motelib AA (1990) Syngenetic and paleokarstic copper mineralization in Paleozoic platform sediments of west central Sinai, Egypt. *BL: sediment hosted mineral deposits. Spec. Publ. Int. Assoc. Sedimentol.*, pp159-170.
- [18]. El Shazly EM, El Hazak NM, Abdel Monem AA, Khawasik SM, Zayed ZM, Mostafa ME, and Morsi MA (1974) Origin of uranium of Oligocene Qatrani sediments, Western Desert, Egypt. *I.A.E.A.*, Vienna.
- [19]. Fernández-Caliani JC, Galán E, Aparicio P, Miras A and Márquez MG (2010) Origin and geochemical evolution of the Nuevo Montecastelo kaolin deposit (Galicia, NW Spain). *Applied Clay Science*, 49: pp91–97.
- [20]. Flinter BH (1959) A magnetic separation of some alluvial minerals in Malaya. *American Mineralogist*, V. 44, No. 7-8, pp738-751.
- [21]. Goldfarb RJ, Groves DI, Gardoll S (2001) Orogenic gold and geologic time: a global synthesis. *Ore Geol. Rev.* 18, pp1–75.

- [22]. Gize AP (2000) The organic geochemistry of gold, platinum and mercury deposits. In: Giordano, T.S., Kettler, R.M., Wodd, S.A. (Eds.), *Ore Genesis and Exploration: The Roles of Organic Matter*. Society of Econ. Geologists, Colorado, pp217–250.
- [23]. Greenwood Philip, Wolfgang Fister, Peter IAKinnell, Hans-Rudolf Rüegg and Nikolaus J Kuhn (2013) Developing and testing a precision erosion measurement facility for elucidating mobilization mechanisms in shallow-flow conditions. *Desertification and Land Degradation*, pp105-111.
- [24]. Gromet LP, Dymek RF, Haskin LA and Korotev RL (1984) The North American shale composite. Its compilation, major and trace elements characteristics. *Geochim. Cosmochim. Acta*, 48; pp2469-2482.
- [25]. Hambleton-Jones BB and Andersen NJB (1984) Natural and induced disequilibrium in surficial uranium deposits. In: *Surficial uranium deposits*, IAEA-TECDOC-322 Vienna, pp 87-93.
- [26]. Hansink JP (1976) Equilibrium analysis of sandstone rollfront uranium deposits. *Proceedings Inter. Symposium on exploration of uranium deposits*. Int. Atomic Energy Agency, Vienna, pp683-693.
- [27]. Haskin LA, Haskin MA, Frey FA and Wildman TR (1968) Relative and absolute terrestrial abundances of the rare earths. In: *Origin and Distribution of the Elements* (Ahrens, L.A., Ed.). Pergamon press. New York, pp 889-912.
- [28]. Heinrich EW (1958) *Mineralogy and geology of radioactive raw materials*. Mc-Graw Hill Book Company, Inc. New York, Toronto, London. 654p.
- [29]. Issawi B, and Jux U (1982) Contribution to the stratigraphy of the Paleozoic rocks in Egypt. *Geol. Surv.*, No.64, 28p.
- [30]. Kora M (1984) The Paleozoic outcrops of Um Bogma area, Sinai. Ph.D. Thesis, Mansoura Univ., Egypt, 280p.
- [31]. Langmuir D (1978) Uranium solution-mineral equilibria at low temperatures with applications to sedimentary ore deposits. *Geochim. Cosmochim. Acta*, 42, pp 547-570.
- [32]. Levinson AA (1980) Introduction to exploration geochemistry Department of geology and geophysics, Univ. of Calgary, Alberta., Canda, Applied Publishing Ltd., Wilmette, Illinois, 601p.
- [33]. Maksimovic Z, Pantó G (1996) Authigenic rare earth minerals in karst-bauxites and karstic nickel deposits. In: Jones, F.A., Wall, F., Williams, C.T. (Eds.), *Rare Earth Minerals, Chemistry, Origin and Ore Deposits*, First Edition. Springer Science and Business Media, pp 257–259.
- [34]. Mansour MGA (1994) Sedimentology and radioactivity of Um Bogma Formation, west central Sinai, Egypt. M.Sc. Thesis, Fac. of Sci., Suez Canal Univ., Ismalia, Egypt. 157p.
- [35]. Mira HI, Shata AE, and El Balakssy SS (2006) Role of microbial action in concentrating uranium and heavy metals within gibbsite mineralization of Um Bogma area, southwestern Sinai, Egypt. 7th Intern. Conf. on Geochemistry, Fac. Sci., Alex. Univ., Alex., Egypt, 6-7 Sept. 2006, V. III, pp 185-203.
- [36]. Omara S, and Conil R (1965) Lower Carboniferous foraminifera from southwestern Sinai, Egypt. *Annals Soc. Geol. Belgique*, 88, pp221-240.
- [37]. Quinif Y, Meon H, Yans J (2006) Nature and dating of karstic filling in the Hainaut Province (Belgium). Karstic, geodynamic and paleogeographic implications. *Geodinamica Acta*. 19, p73-85.
- [38]. Said R (1971) Explanatory notes to accompany the geologic map of Egypt. *Geol. Surv. Egypt*, V. 56, 123p.
- [39]. Sallam OR, Alshami AS, Mohamed SA and El Akeed IA (2014) The Occurrence of silver-gold mineralization associated with uranium bearing minerals and base metal sulphide, El Sheikh Soliman Area, South Sinai, Egypt. *Egy. J. Pure & Appl. Sci.* 2014, V. 52(1), pp47-54.
- [40]. Shapiro L and Branock WW (1962) Rapid analysis of silicate, carbonate and phosphate rocks. *U. S. Geol. Surv., Bull.*, 114(A): 56p.
- [42]. Soliman MS and Abu El Fetouh MA (1969) Petrology of Carboniferous and sandstone in West Central Sinai, Egypt. *J. Geol. UAR*, V. 13, pp43-61.
- [43]. Taylor SR and McLennan SM (1981) The Composition and Evolution of the Continental-Crust - Rare-Earth Element Evidence from Sedimentary-Rocks. *Philosophical Transactions of the Royal Society of London* 301(1461), pp 381-399.
- [44]. Weissbrod T (1969) The Paleozoic outcrops in South Sinai and their correlation with those of southern Israel. In: *The Paleozoic of Israel and adjacent countries*. *Bull. Geol. Surv.*, V. 2, pp17-32.
- [45]. (<https://en.wikipedia.org/wiki/Autunite>)
- [46]. (<https://en.wikipedia.org/wiki/Zircon>)

Osama R. Sallam. "Factors Controlling in the Concentration of Gold, Uranium and some Base Metals in the Lower Carboniferous Marl at Wadi El Kharig area, Southwestern Sinai, Egypt." *IOSR Journal of Applied Geology and Geophysics (IOSR-JAGG)*, 8(2), (2020): pp. 07-22.